Combined EUV reflectance and X-ray reflectivity data analysis of periodic multilayer structures

S. N. Yakunin,[1,*] I. A. Makhotkin,[2,3] K. V. Nikolaev,[1] R. W. E. van de Kruijs,[2,3] M. A. Chuev,[4] and F. Bijkerk[2,3]

[1]NRC Kurchatov Institute, Moscow, Russia
[2]MESA+, Institute for Nanotechnology, University of Twente, Netherlands
[3]FOM Institute DIFFER, Nieuwegein, Netherlands
[4]IPT RAS, Moscow, Russia
[*]s.n.yakunin@gmail.com

Abstract: We present a way to analyze the chemical composition of periodical multilayer structures using the simultaneous analysis of grazing incidence hard X-Ray reflectivity (GIXR) and normal incidence extreme ultraviolet reflectance (EUVR). This allows to combine the high sensitivity of GIXR data to layer and interface thicknesses with the sensitivity of EUVR to the layer densities and atomic compositions. This method was applied to the reconstruction of the layered structure of a LaN/B multilayer mirror with 3.5 nm periodicity. We have compared profiles obtained by simultaneous EUVR and GIXR and GIXR-only data analysis, both reconstructed profiles result in a similar description of the layered structure. However, the simultaneous analysis of both EUVR and GIXR by a single algorithm lead to a ~2x increased accuracy of the reconstructed layered model, or a more narrow range of solutions, as compared to the GIXR analysis only. It also explains the inherent difficulty of accurately predicting EUV reflectivity from a GIXR-only analysis.

© 2014 Optical Society of America

OCIS codes: (340.6720) Synchrotron radiation; (340.7470) X-ray mirrors; (340.7480) X-rays, soft x-rays, extreme ultraviolet (EUV).

References and links

1. E. Louis, A. E. Yakshin, T. Tsarfati, and F. Bijkerk, "Nanometer interface and materials control for multilayer EUV–optical applications," Prog. Surf. Sci. **86**, 255–294 (2011).
2. M. G. Pelizzo, M. Suman, G. Monaco, P. Nicolosi and D. L. Windt, "High performance EUV multilayer structures insensitive to capping layer optical parameters," Opt. Express **16**, 15228–15237 (2008).
3. M. H. Hu, K. Le Guen, J. M. André, P. Jonnard, E. Meltchakov, F. Delmotte, and A. Galtayries, "Structural properties of Al/Mo/SiC multilayers with high reflectivity for extreme ultraviolet light," Opt. Express **18**, 20019–20028 (2010).
4. Q. Zhong, Z. Zhang, J. Zhu, Z. Wang, P. Jonnard, K. Le Guen, and T. Huo, "The thermal stability of Al (1% wtSi)/Zr EUV mirrors," Appl. Phys. A **109**, 133–138 (2012).
5. K. Le Guen, M. H. Hu, J. M. André, P. Jonnard, S. K. Zhou, H. C. Li and C. Meny, "Development and interfacial characterization of Co/Mg periodic multilayers for the EUV range," J. Phys. Chem. C **114**, 6484–6490 (2010).
6. S. Braun, R. Dietsch, M. Haidl, T. Holz, H. Mai, S. Müllender, and R. Scholz, "Mo/Si-multilayers for EUV applications prepared by Pulsed Laser Deposition (PLD)," Microelectron. Eng. **57**, 9–15 (2001).
7. S. Andreev, M. Barysheva, N. Chkhalo, S. Gusev, A. Pestov, V. Polkovnikov, D. Rogachev, N. Salashchenko, Y. A. Vainer, and S. Y. Zuev, "Multilayer X-ray mirrors based on La/B4C and La/B9C," Tech. Phys. **55**, 1168–1174 (2010).

8. I. A. Makhotkin, E. Zoethout, R. van de Kruijs, S. N. Yakunin, E. Louis, A. M. Yakunin, V. Banine, S. Müllender, and F. Bijkerk, “Short period La/B and LaN/B multilayer mirrors for 6.8 nm wavelength,” Opt. Express **21**, 29894–29904 (2013).
9. I. A. Makhotkin, R. van de Kruijs, E. Zoethout, E. Louis and F. Bijkerk, “Optimization of LaN/B multilayer mirrors for 6.x nm wavelength,” SPIE Optical Engineering+ Applications. – International Society for Optics and Photonics (2013).
10. M. Born and E. Wolf, *Principles of Optics* (Cambridge University, 1999).
11. J. Daillant and A. Gibaud, *X-ray and Neutron Reflectivity: Principles and Applications*, vol. 770 of *Lecture Notes in Physics* (Springer, 2009).
12. L. D. Landau and E. M. Lifshitz, *Electrodynamics of Continuous Media*, vol. 8 of *Course of Theoretical Physics* (ButterworthHeinemann, 1984).
13. V. G. Kohn, “On the theory of reflectivity by an x-ray multilayer mirror,” Phys. Status Solidi (b) **187**, 61–79 (1995).
14. K. Stoev and K. Sakurai, “Recent theoretical models in grazing incidence X-ray reflectometry,” The Rigaku J. **14**, 22–37 (1997).
15. B. L. Henke, E. M. Gullikson, and J. C. Davis, “X-ray interactions: photoabsorption, scattering, transmission, and reflection at E=50-30000 eV, Z=1-92,” Atomic Data and Nuclear Data Tables **54**, 181–342 (1993).
16. V. G. Kohn, “On the theory of X-ray reflectivity by multilayer mirrors. Debye–Waller and Nevot–Croce approximations for taking into account the roughness of interfaces (in russian),” J. Surf. Invest.: X-Ray, Synchrotron Neutron Tech. **1**, 23–27 (2003).
17. A. Gibaud and S. Hazra, “X-ray reflectivity and diffuse scattering,” Curr. Sci. **78**, 1467–1477 (2000).
18. I. G. Hughes and T. P. A. Hase, *Measurements and Their Uncertainties* (Oxford University, 2010).
19. A. Afanas’ev and M. Chuev, “Discrete forms of Mössbauer spectra,” J. Exp. Theor. Phys. **80**, 560–567 (1995).
20. G. A. Korn and T. M. Korn, *Mathematical Handbook for Scientists and Engineers: Definitions, Theorems, and Formulas for Reference and Review* (General Publishing Company, 2000).
21. T. Tsarfati, R. van de Kruijs, E. Zoethout, E. Louis, and F. Bijkerk, “Nitridation and contrast of B4C/La interfaces and X-ray multilayer optics,” Thin Solid Films **518**, 7749–7752 (2010).
22. F. Scholze, J. Tmmler, and G. Ulm, “High-accuracy radiometry in the EUV range at the PTB soft X-ray beamline,” Metrologia **40**, 224–228 (2003).
23. J. Tümmler, H. Blume, G. Brandt, J. Eden, B. Meyer, H. Scherr, F. Scholz, F. Scholze, and G. Ulm, “Characterization of the PTB EUV reflectometry facility for large EUVL optical components,” Proc. SPIE **5037**, 256–273 (2003).
24. F. Scholze, C. Laubis, C. Buchholz, A. Fischer, S. Plöger, F. Scholz, and G. Ulm, “Polarization dependence of multilayer reflectance in the EUV spectral range,” Proc. SPIE **6151**, 615137 (2006).
25. I. A. Makhotkin, E. Zoethout, E. Louis, A.M. Yakunin, S. Müllender and F. Bijkerk, “Spectral properties of La/B – based multilayer mirrors near the boron K absorption edge,” Opt. Express **20**, 11778–11786 (2012).
26. M. Fernández-Perea, J. I. Larruquert, J. A. Aznárez, J. A. Méndez, M. Vidal-Dasilva, E. Gullikson, A. Aquila, R. Soufli, J. L. G. Fierro, “Optical constants of electron-beam evaporated boron films in the 6.8-900 eV photon energy range,” J. Opt. Soc. Am. A **24**, 3800–3807 (2007).

---

1. Introduction

Layered materials find many applications nowadays. These range from nanomaterials in general to XUV reflecting Bragg optics, also down to atomic scale dimensions [1]. Traditional characterization of such, periodic multilayer mirrors usually involves two types of measurements of the reflectance, one performed using hard x-rays at grazing incidence (GIXR), and a second performed at an application relevant wavelength. A structural model obtained from hard x-ray reflectometry analysis is generally not able to accurately predict the application relevant reflectivity data. The reason for this, as will be shown in this article, is that the reflectivities at different wavelengths have different sensitivities to the multilayer structural parameters. For example, while hard x-rays are very sensitive to the layer thicknesses in the multilayer period, it is less sensitive to the chemical composition of the layers. Soft x-rays are extremely sensitive to the compositional parameters of the layers, such as stoichiometry and the presence of impurity atoms, but the analysis of such data suffers from the large correlation between model parameters that describe the measurement curves.

There are a number of publications [2, 3, 4] where authors attempted to use GIXR and other techniques for the explanation of EUVR data. Almost in all papers authors mention poor agreement between experimental data and calculations of EUV reflectivity curves, based on the mul-

tilayer structural model obtained from GIXR data analysis. In [5] authors explain this poor agreement by the inaccurate optimization of multilayer parameters during GIXR data analysis. A more satisfactory agreement between structural models obtained from GIXR and EUVR data was presented by Braun et.al. in [6]. The reason for this good agreement is that authors have added information about the structure of the interface layers as obtained from high resolution TEM to the initial models for GIXR data fitting, significantly improving the fitting procedure, but at the expense of an additional multilayer characterization process. A recent attempt to obtain a consistent model of a multilayer period structure that describes both hard x-ray reflectivity (GIXR, 0.154 nm) and extreme ultraviolet reflectivity (EUVR, ~6.7 nm) measurements is discussed in [7]. In that article authors have analyzed sequentially GIXR and EUVR data, concluding that interface roughness values for the model that describes EUVR should be higher than interface roughness values for the model that describes GIXR data. One of the possible reasons of inconstancy between these models was attributed to neglecting the atomic composition of diffused layers. Therefore we observe the need for a set of mathematical procedures for combined analysis of GIXR and EUVR data.

In this article we will discuss simultaneous fitting of GIXR and EUVR data using a single model that simultaneously describes both sets of data. This approach is expected to result in a reliable and accurate model of the multilayer structure that provides more accurate information about the internal structure, as well as enabling a more accurate prediction of the reflectivity of multilayers with changing model parameters such as a variation of the multilayer period thickness or a variation of the number of periods as discussed in [8, 9]. In order to account for the different sensitivities of X-rays and EUV radiation to the chemical composition of the layers, we propose to add the chemical composition of layers and interfaces as a parameters during the combined fit of GIXR and EUVR data.

Basic mathematical techniques optimized for the simulation of reflectivity data for a periodic multilayer structure are discussed. To study the benefits of using several sets of data for the reconstruction of the material parameters such as densities and atomic compositions of layers, we have performed an extensive analysis of errors of the reconstructed optical constants profiles and correlations between fit parameters. To illustrate the performance of a combined GIXR and EUVR analysis, we analyzed a LaN/B multilayer optimized for normal incidence reflectivity at a wavelength of 6.8 nm and discuss reconstructed profiles from GIXR-only and from combined GIXR and EUVR analysis. This material combination is of particular interest because of its current application as spectroscopic element in XRF analysis equipment and its potential application as reflective optical element in next generation EUV photolithography.

2. Modeling of reflectivity from periodic multilayer structures

In this part we present a brief description of electromagnetic wave propagation, optimized for fast calculation of the reflectivity from a periodic multilayer structure. The wave propagation in a homogeneous layer can be characterized using the transfer matrix [10] M_i that connects the electric field and its first derivative at the interfaces between neighboring layers i and $i+1$:

$$\mathsf{M}_i = \begin{pmatrix} \cos k_{z,i} d_i & 1/k_{z,i}\ \sin k_{z,i} d_i \\ -k_{z,i} \sin k_{z,i} d_i & \cos k_{z,i} d_i \end{pmatrix}, \tag{1}$$

where d_i is the layer thickness and $k_{z,i}$ is a projection of the wave vector on to the z-direction in layer i. In general case, $k_{z,i}$ depends on the polarization [11] of the incident radiation:

$$k_{z,i} = \begin{cases} k_0 \sqrt{n_i^2 - n_0^2 \cos^2\theta} & \text{s polarization,} \\ k_0 n_i^2 / \sqrt{n_i^2 - n_0^2 \cos^2\theta} & \text{p polarization;} \end{cases} \tag{2}$$

#213049 15.00 USD Received 29 May 2014; revised 21 Jul 2014; accepted 23 Jul 2014; published 12 Aug 2014
(C) 2014 OSA

where $n_i = 1 - \delta_i - i\beta_i$ is the complex refractive index inside layer i [12], $k_0 = |\mathbf{k}_0| = 2\pi/\lambda$ is the absolute value of the wave vector in vacuum, λ is the incident beam wavelength and θ is the grazing incident angle.

The wave propagation through a system with N layers is then represented by the characteristic matrix:

$$\mathsf{M} = \mathsf{M}_N \mathsf{M}_{N-1} \cdots \mathsf{M}_2 \mathsf{M}_1 = \prod_{i=N}^{1} \mathsf{M}_i. \quad (3)$$

For periodic multilayer structures with identical periods, the multiplication of matrices M_i can be calculated via the exponentiation formula [10]:

$$\widetilde{\mathsf{M}}^K = \begin{pmatrix} \tilde{m}_{11} & \tilde{m}_{12} \\ \tilde{m}_{21} & \tilde{m}_{22} \end{pmatrix}^K = \begin{pmatrix} \tilde{m}_{11} U_{K-1}(a) - U_{K-2}(a) & \tilde{m}_{12} U_{K-1}(a) \\ \tilde{m}_{21} U_{K-1}(a) & \tilde{m}_{22} U_{K-1}(a) - U_{K-2}(a) \end{pmatrix}. \quad (4)$$

Here $U_K(a) = \sin[(K+1)\arccos a]/\sqrt{1-a^2}$ is the Chebyshev polynomial of the second kind [13], where $a = 1/2(\tilde{m}_{11} + \tilde{m}_{22})$, $\widetilde{\mathsf{M}}$ is the characteristic matrix calculated for a multilayer period and K is the number of periods in a multilayer structure. This approach is valid for unimodular matrices and can be applied to the characteristic matrices discussed here because $\det(\mathsf{M}_i) = 1$. Using Chebyshev polynomials allows to save computational resources, proportionally to the number of periods in a multilayer stack in comparison with standard matrix multiplication procedures in Eq. (3).

The reflectance amplitude is now given by [10]:

$$r = \frac{k_{z,N+1} k_{z,0} M_{12} + i k_{z,0} M_{22} - i k_{z,N+1} M_{11} + M_{21}}{k_{z,N+1} k_{z,0} M_{12} + i k_{z,0} M_{22} + i k_{z,N+1} M_{11} - M_{21}}, \quad (5)$$

where $k_{z,0}$ and $k_{z,N+1}$ are the wave vector projections in ambient and substrate media respectively. Reflected beam intensity can then be calculated by:

$$I^{\text{calc}}(\theta, \lambda, \mathbf{p}) = |r|^2 I_0, \quad (6)$$

where $\mathbf{p}$ is the set of structural parameters (layer thicknesses and refractive indices) and I_0 is the incident beam intensity. Formulas Eq. (1) – Eq. (6) will further be used for model simulations of GIXR and EUVR curves.

3. Parameterization of a multilayer structure

For simulations analysis of GIXR and EUVR data, Eq.(6) can be written as

$$I = \begin{cases} I^{\text{calc}}_{\text{GIXR}}(\theta, \lambda, \mathbf{p})\big|_{\lambda=\lambda_0}, \\ I^{\text{calc}}_{\text{EUVR}}(\theta, \lambda, \mathbf{p})\big|_{\theta=\theta_0}; \end{cases} \quad (7)$$

where λ_0 is a fixed wavelength used for the measurements of GIXR, and θ_0 is a fixed angle used for measurements of EUVR. According to Eq. (1) – Eq. (6), a multilayer is described by a set of individual layers with thicknesses d_i and complex refractive indices n_i.

The refractive index of the i–th layer ($n_i = 1 - \delta_i - i\beta_i$) depends on it's chemical composition and density according to [14]:

$$\begin{aligned} \delta_i &= 2.7007 \times 10^{-4} \times \tfrac{\rho_i \lambda^2}{\mu_i} \sum_{j=1}^{\Omega_i} \omega_{ij} f_j^{(1)}(\lambda), \\ \beta_i &= 2.7007 \times 10^{-4} \times \tfrac{\rho_i \lambda^2}{\mu_i} \sum_{j=1}^{\Omega_i} \omega_{ij} f_j^{(2)}(\lambda). \end{aligned} \quad (8)$$

#213049 15.00 USD Received 29 May 2014; revised 21 Jul 2014; accepted 23 Jul 2014; published 12 Aug 2014
(C) 2014 OSA

Here ρ_i is the density in $[\mathrm{g/cm^3}]$, μ_i is the molar weight of a compound in [g/mol] with Ω_i different atomic species, ω_{ij} is the atomic concentration of atoms j in layer i, and f_j is the atomic scattering factor for atomic species j [15].

Although $\mathbf{p}$ contains the thicknesses needed to describe the layered model for reflectivity simulations, periodic multilayer mirrors are often described using technological parameters such as period thickness D and layer thickness ratio Γ instead of the individual layer thicknesses d_i. In analogy to the technological parameters D and Γ we introduce the relative (to the period) interface imperfections parameter S and the interface imperfections ratio parameter S_Γ. Thus for a two-layer model, it is convenient to use a set of effective parameters:

$$\begin{cases} D = d_1 + d_2 + \sigma_1 + \sigma_2, \\ \Gamma = (2d_2 + \sigma_1 + \sigma_2)/2D, \\ S = (\sigma_1 + \sigma_2)/D, \\ S_\Gamma = \sigma_2/(\sigma_1 + \sigma_2). \end{cases} \tag{9}$$

Interface imperfections between layers i and $i+1$, resulting from intermixing and/or surface roughness over a depth range of σ_i, effectively create a gradual change in δ and β from layer i to layer $i+1$. This gradual change is taken into account in the model by replacing this depth range σ_i by a finite set of layers with total thickness σ_i that introduce a gradual stepwise profile from δ_i to δ_{i+1} and from β_i to β_{i+1} [16]. Here the profile is chosen according to a sinusoidal distribution of optical characteristics between homogeneous media. This approach maintains the continuity of the electric field at the interfaces and properly considers dynamic effects, unlike the commonly used DebyeWaller or NevotCroce statistical factors [11, 17]. Also it takes into account the shift of the diffraction peaks caused by interface imperfections. Furthermore this description of the interfaces does not affect the unimodularity condition for the characteristic matrix Eq. (1), and therefore allows the application of the exponentiation formula Eq. (4).

4. Reconstruction and error analysis of structural parameters

The reconstruction of the structural parameters is formulated as an optimization problem [18]:

$$\tilde{\mathbf{p}} = \min_{\mathbf{p}} \chi^2(\mathbf{p}), \tag{10}$$

where $\tilde{\mathbf{p}}$ is a resulting set of reconstructed parameters and χ^2 is a goodness of fit value similar to Pearson's criterion.

In order to reconstruct parameters from two sets of experimental data the criterion for fit goodness has the form:

$$\chi^2 = \frac{1}{L_{\mathrm{GIXR}} + L_{\mathrm{EUVR}} - l} \left[\sum_\theta \frac{\left(I^{\mathrm{calc}}_{\mathrm{GIXR}}(\theta, \mathbf{p})\big|_{\lambda=\lambda_0} - I^{\mathrm{exp}}_{\mathrm{GIXR}}(\theta) \right)^2}{\sigma^2_{\mathrm{GIXR}}(\theta)} + \sum_\lambda \frac{\left(I^{\mathrm{calc}}_{\mathrm{EUVR}}(\lambda, \mathbf{p})\big|_{\theta=\theta_0} - I^{\mathrm{exp}}_{\mathrm{EUVR}}(\lambda) \right)^2}{\sigma^2_{\mathrm{EUVR}}(\lambda)} \right], \tag{11}$$

where L_{GIXR} and L_{EUVR} are numbers of measured data points, l is the number of parameters that are used to describe the layered structure, and σ_{GIXR} and σ_{EUVR} are the uncertainties in the measured GIXR and EUVR data respectively. Both σ_{GIXR} and σ_{EUVR} are calculated according to $\sigma^2(\theta) = \sigma^2_{\mathrm{sys}} + \sigma^2_{\mathrm{stat}}$, where σ_{sys} is a systematic error that relates to uncertainties in the measurement setup, and σ_{stat} is the statistical error in the measured data relates to the discrete nature of radiation. If errors in the experimental data are normally distributed and the number of experimental points is much larger than the number of fit parameters, a goodness of fit for a perfect model has a value of $\chi^2 = 1$.

In order to solve the optimization problem of Eq. (10), a Levenberg-Marquardt algorithm is used [18]. Standard deviations of reconstructed parameters Δp_i are calculated by the least

#213049 15.00 USD Received 29 May 2014; revised 21 Jul 2014; accepted 23 Jul 2014; published 12 Aug 2014
(C) 2014 OSA

squares method [19]. To estimate standard deviations the covariance matrix is used [20]:

$$C_{ij} = \mathrm{cov}(p_i, p_j) = \left[\sum_{k=1}^{L} \frac{1}{\sigma_k^2} \frac{\partial I_k}{\partial p_i} \frac{\partial I_k}{\partial p_j} \right]^{-1}. \tag{12}$$

In case of simultaneous analysis of GIXR and EUVR data the concatenation of two experimental data sets is taken into account in Eq. (12). Consequently $I = (I_{\mathrm{GIXR}}, I_{\mathrm{EUVR}})$ is a cumulative set of measured data, $\sigma = (\sigma_{\mathrm{GIXR}}, \sigma_{\mathrm{EUVR}})$ is a cumulative error, and $L = L_{\mathrm{GIXR}} + L_{\mathrm{EUVR}}$ is the total number of data points. Structural parameters p_i are considered as normally distributed random variables to obtain standard deviations:

$$\Delta p_i = \sqrt{C_{ii}}. \tag{13}$$

The degree of linear dependency of the parameters is determined by the matrix of Pearson correlation coefficients [18]:

$$R_{ij} = \frac{C_{ij}}{\sqrt{C_{ii} C_{jj}}}. \tag{14}$$

Elements of matrix R are ranging from -1 to 1. As an example a large absolute value of correlation coefficient $|R_{ij}|$ implies a large dependence between structural parameters p_i and p_j. If $R_{ij} > 0$, an increase of parameter p_i can be compensated by an increase of parameter p_j and vice versa, keeping the same χ^2 value. If $R_{ij} < 0$, an increase of parameter p_i can be compensated by a decrease of the parameter p_j and vice versa.

Based on the reconstructed parameters of the structure, one can obtain the depth distribution of the dispersion parameter $\delta(z)$. For the analysis of $\delta(z)$ the uncertainties correlation analysis is used:

$$\varepsilon(z) = \left[\sum_i \left(\frac{\partial \delta(z)}{\partial p_i} \right)^2 C_{ii} + 2 \sum_{i>j} \left(\frac{\partial \delta(z)}{\partial p_i} \frac{\partial \delta(z)}{\partial p_j} \right) C_{ij} \right]^{1/2}. \tag{15}$$

5. Experiment layout and data processing

A simultaneous analysis of GIXR and EUVR was performed for a 50 period LaN/B multilayer. Both La and B were deposited using DC magnetron sputtering. The LaN layer was created using nitrogen assisted growth similar to the approach described in [21]. The layer thicknesses were controlled by pre-calibrated deposition rates.

For the detailed analysis of the accuracy of the measurements it is essential to take all uncertainties into account. Unlike statistical error which strictly depends on experimental data, a systematic error is included that arises from the specific geometry of experimental setup.

The hard X-ray reflectivity measurements were carried out on a laboratory difractometer (PanAlytical Empyrean) using the characteristic $\mathrm{CuK}_{\alpha 1}$ radiation with a wavelength of $\lambda = 0.15406\,\mathrm{nm}$. The monochromatization and primary collimation of the incident beam was done using a four bounce asymmetricaly cut germanium monochromator which gives a beam divergence of $\Delta\theta \approx 0.015^\circ$. For the calculation of errors we have also taken into account the fluctuation of the direct beam within — 2.5% of intensity, and possible errors in determination of incidence angle of $\Delta\theta \approx 0.017^\circ$.

The geometry of the experimental scheme, the cross section of the beam and the sample size were used for calculation of geometrical effects near the angle of total external reflection for GIXR data analysis.

The measurement of EUV reflectivity was performed at PTB (Physikalisch Technische Bundesanstal) [22, 23, 24]. The accuracy of measurement was: intensity stability — 0.02%; fluctuations in the detector — 0.04%; the presence of high-order harmonics — 0.02%; diffusely scattered radiation — 0.08%. The total systematic error did not exceed 0.1%.

#213049 15.00 USD Received 29 May 2014; revised 21 Jul 2014; accepted 23 Jul 2014; published 12 Aug 2014
(C) 2014 OSA

To reconstruct the multilayer structure, the calculations of GIXR and EUVR data were fitted to the measured data. Initially only GIXR data were fitted, having effective parameters Eq. (9) and layer densities as free parameters. The fit model consisted of 49 periods with identical parameters and one additional top period with independent parameters to account for the effect of surface contamination (e.g. oxidation). The best fit model from GIXR analysis was subsequently used as the initial model for the simultaneous fit of GIXR and EUVR data, where the material compositions of layers are added as additional fit parameters.

For the analysis of a LaN/B multilayer, the LaN layer composition is defined as $(\mathrm{LaN})_{\omega_{\mathrm{LaN}}}\mathrm{B}_{1-\omega_{\mathrm{LaN}}}$ and the B layer composition is defined as $\mathrm{B}_{\omega_{\mathrm{B}}}(\mathrm{LaN})_{1-\omega_{\mathrm{B}}}$. Especially for a wavelength in the vicinity of the B K_α absorption edge the EUVR simulations are very sensitive to the B optical constants [25, 26] and therefore to the B layer composition. For calculations of EUVR measured boron optical constants were used [26].

To estimate uncertainties in reconstructed parameters, standard deviations of fit parameters were calculated according to Eq. (13). Matrices of Pearson correlation coefficients are calculated for GIXR, EUVR and cumulative fits using Eq. (14), in order to analyze the stability of the solution of the optimization problem. The correlation matrix is calculated separately for each experiment to analyze sensitivity of the various experimental techniques to the parameters of the structure.

6. Results

The results of GIXR-only fitting are shown in Fig. 1 and the parameters of best fit models are presented in Table 1. Figure 1 shows experimental data and best fit calculations, as well as the residuals $u = (I_{\mathrm{exp}} - I_{\mathrm{calc}})/\sigma$. The good agreement between fit calculations and experimental data can be recognized from the residuals that stay well within a range of $(-3 \div 3)$, and the fit quality value of $\chi^2 = 1.01$.

Figure 2 shows measured and calculated EUVR curves. The dashed reflectivity curve was calculated based on the model obtained after the GIXR-only fit. Although the GIXR curve was fitted almost perfectly, the calculated EUVR curve does not fit to the measurements at all. It is clear that the structure parameters obtained from a GIXR-only fit are not sufficient to predict the multilayer characteristics in the EUV range.

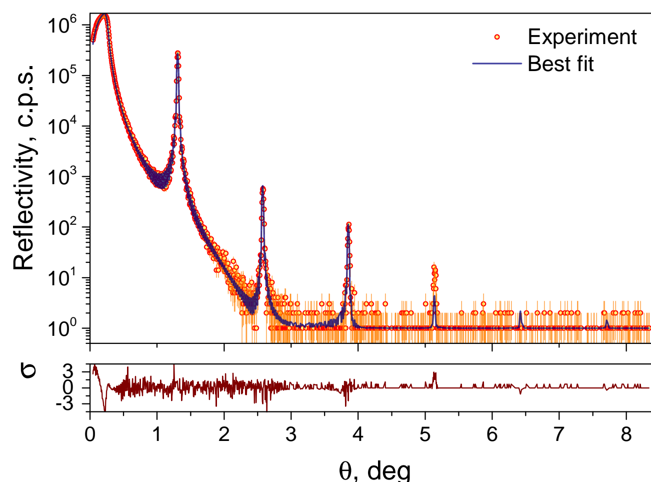

Fig. 1. Calculated and measured GIXR curves for a LaN/B multilayer (top section), and the fit residuals (bottom section).

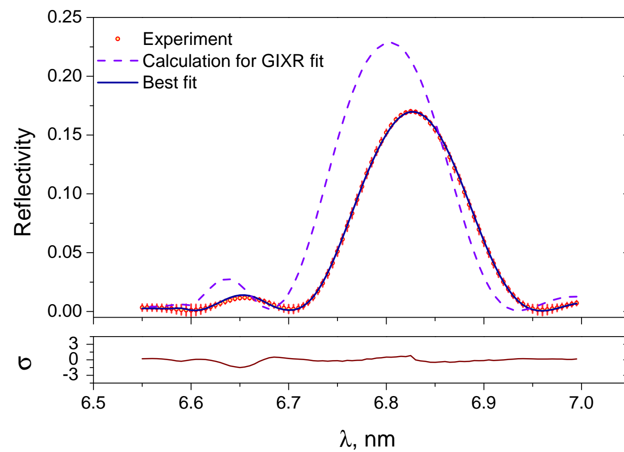

Fig. 2. Calculated (see text for details) and measured curves for EUVR fit (top section) and the residual between best fit solution and the measured data (bottom section).

When a simultaneous analysis of GIXR and EUVR data is performed, the EUVR data can be reproduced accurately, as shown in Fig. 2 (solid line). The fit quality of the GIXR data, as obtained from the simultaneous GIXR and EUVR analysis, remained similar to that shown in Fig. 1. Resulting fit parameters from the simultaneous analysis are also shown in Table 1.

Table 1. Resulting model of the periodic structure

	GIXR	Simultaneous
D, nm	3.432 ± 0.001	3.434 ± 0.001
Γ	0.542 ± 0.005	0.529 ± 0.004
S	0.85 ± 0.01	0.846 ± 0.006
S_Γ	0.529 ± 0.007	0.573 ± 0.005
ρ_{B}, g/cm^3	2.7 ± 0.2	2.94 ± 0.07
ρ_{LaN}, g/cm^3	5.4 ± 0.6	5.58 ± 0.14
ω_{B}	1.00 ± 0.04	0.977 ± 0.002
ω_{LaN}	1.0 ± 0.7	1.00 ± 0.03

To explore the discrepancy between the calculated EUVR response from GIXR-only and simultaneous GIXR and EUVR analysis, the δ-profiles and their tolerance areas were calculated, based on the parameters presented in Table 1. The tolerance areas are calculated using Eq. (15). The δ-profiles and their tolerance areas were calculated for two wavelengths: 0.15 nm and 6.8 nm. The δ-profiles calculated for a wavelength of 0.15 nm are indicated as δ_{CuK} in Fig. 3(a). Profiles that are calculated for a wavelength of 6.8 nm are indicated as δ_{EUV} in a Fig. 3(b). The profiles that were calculated for a structural model obtained from the GIXR-only analysis will be referred to further as $\delta^{\mathrm{G}}_{\mathrm{CuK}}$ and $\delta^{\mathrm{G}}_{\mathrm{EUV}}$, while the profiles that correspond to the simultaneous GIXR and EUVR analysis will be referred to as $\delta^{\mathrm{S}}_{\mathrm{CuK}}$ and $\delta^{\mathrm{S}}_{\mathrm{EUV}}$.

The profiles can be divided into two types of regions, one region where the value of δ is constant, related to the thicknesses d_1 and d_2 of the LaN and B layers respectively, and another region where a gradual transition of δ occurs between the LaN and B layers and between the B and LaN layers, corresponding to the interface widths σ_1 and σ_2, respectively.

#213049 15.00 USD Received 29 May 2014; revised 21 Jul 2014; accepted 23 Jul 2014; published 12 Aug 2014
(C) 2014 OSA

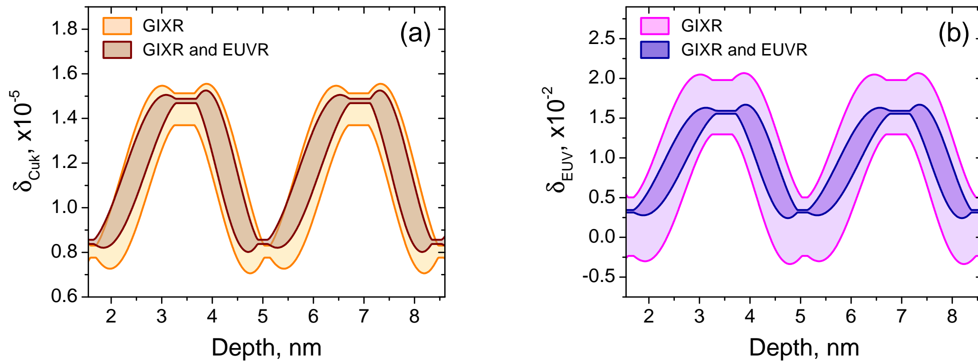

Fig. 3. Tolerance areas of δ-profiles of double period, calculated for 0.154 nm (a) and 6.8 nm (b) obtained for GIXR data fit (light) and cumulative GIXR and EUVR fit (dark).

7. Discussion

The comparison of $\delta^{G}_{\rm CuK}$ and $\delta^{S}_{\rm CuK}$ profiles as plotted in Fig. 3(a) explains why the fit quality of GIXR was not changed. The solution of the simultaneous fit stays within the tolerance corridor of the solution of the GIXR-only fit. In Fig. 3(a) we can also see that the introduction of EUVR data into the analysis strongly increases the accuracy of the determination of optical constants, in particular at the position of the La and B layers. Table 1 shows that after the simultaneous fit, the error in the determination of densities decreases significantly.

The comparison of $\delta^{G}_{\rm EUV}$ and $\delta^{S}_{\rm EUV}$ profiles shows that within the tolerance corridor of the $\delta^{G}_{\rm EUV}$, a large variety of optical profiles calculated for 6.8 nm wavelength can be placed. The tolerance corridor of $\delta^{S}_{\rm EUV}$ is dramatically narrower than that of $\delta^{G}_{\rm EUV}$.

The $\delta^{G}_{\rm EUV}$ profile, which corresponds to the best fit model of GIXR-only analysis, does not fit into the $\delta^{S}_{\rm EUV}$ corridor, which explains the poor prediction of EUVR data from the GIXR-only analysis as shown in Fig. 2. The main reason for the large tolerance regions of $\delta^{G}_{\rm EUV}$ is that a variation of $\omega_{\rm LaN}$, $\omega_{\rm B}$, $\rho_{\rm LaN}$ and $\rho_{\rm B}$ parameters would lead to only a small change in $\delta_{\rm CuK}$ while leading to much larger changes in $\delta_{\rm EUV}$.

Figure 4 shows the errors of the determined parameters as well as Pearson's correlation coefficient matrices, calculated using Eq. (14), for the GIXR (a), EUVR (b) and simultaneous (c) GIXR and EUVR analysis. Although we did not fit EUVR curves separately, we have calculated errors of possible EUVR-only fit for discussions. From Fig. 4a it can be concluded that the effective parameters (D,Γ,S and S_Γ) are determined with high accuracy from the GIXR-only fit. Specifically the period D of the multilayer mirror can be determined within an uncertainty of $\varepsilon D \approx 0.01\%$. This high accuracy can be explained due to the fact that D is strongly associated with the angular positions of the diffraction peaks, where a slight change in D leads to a large change in χ^2. As shown in Fig. 4(a) the parameter D is only weakly correlated with other parameters. This is due the fact that shifting peaks position cannot be compensated by the change of other structural parameters.

Effective parameters Γ,S and S_Γ determine the shape of the $\delta_{\rm CuK}$-profile which determines the intensity ratio of the diffraction peaks. The accuracy with which these parameters can be determined from the GIXR analysis alone is typically in the order of $\varepsilon \approx 0.1\%$. One can notice that the correlation between Γ, S and S_Γ is much larger than between D and the other parameters. This is related to the fact that a change in the layer asymmetry parameter Γ can be partially compensated by a change in the interface parameters S and S_Γ. This large correlation explains the large tolerance areas in the interface regions of $\delta_{\rm CuK}$, and indicates that GIXR-only data

#213049 15.00 USD Received 29 May 2014; revised 21 Jul 2014; accepted 23 Jul 2014; published 12 Aug 2014
(C) 2014 OSA

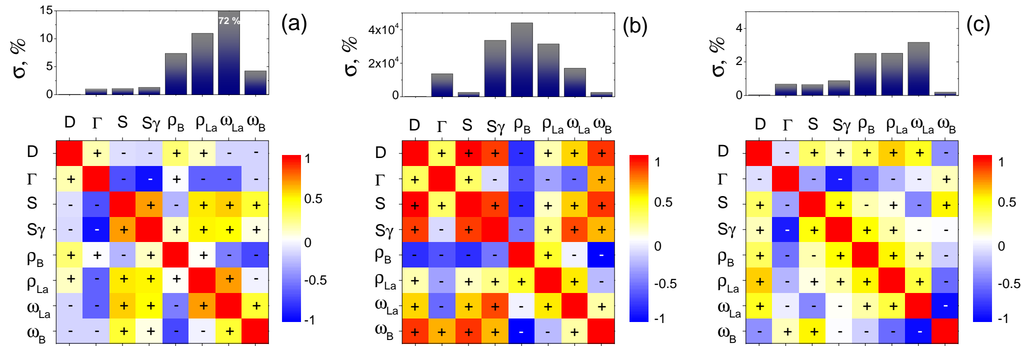

Fig. 4. (top section) The relative errors of structural parameters. (bottom section) Matrices of Pearson's correlation coefficients. (left) for GIXR, (middle) for EUVR and (right) for simultaneous optimization.

analysis is not sensitive to the exact shape of δ-profile in the interface regions. In effect, the same fit goodness can be achieved with a linear or Gaussian interface shape instead of the sinusoidal shape that was used in the analysis. To increase the sensitivity to the interface shape, reflectivity information from a much larger measured angular range is required. For GIXR reflectivity the minimal resolvable feature can be estimated by the formula $\delta z = \lambda/2\pi \sin\theta_{\max}$, were $\theta_{\max}$ is the maximal measured angle. For the measurements presented here $\theta_{\max} = 5^{\circ}$, therefore the resolution of the optical contrast profile determination is limited by 0.3 nm.

Figure 3(a) and Table 1 show that the addition of EUVR data to the reflectivity analysis does not significantly increase the accuracy of determination of Γ and S_{Γ}. This is primarily because of the high correlations between S and S_{Γ} for EUVR data as showed on Fig. 4(b). However the error of determination S was reduced by a factor two as a result of the simultaneous data analysis of the EUV and X-ray range. Figure 4(b) shows that the EUVR-only analysis would not provide accurate information about multilayer structure because of the large correlation between parameters.

The analysis of correlated errors in simultaneous EUVR and GIXR data analysis showed only a minor decrease of the correlation coefficients as compared to the GIXR-only analysis. However, the simultaneous analysis does significantly increase the accuracy of the determination of the optical constants of the layers in the multilayer structure. According to the Table 1, the largest increase of sensitivity was observed for the determination of the density of the LaN layer (ρ_{LaN}) and for the determination of the LaN atomic fraction in B layer (ω_{B}). The reason for it is the sensitivity of EUVR data to the optical contrast between spacer and reflector layers in the multilayer. A reduction of the LaN layer density and an increase of the B layer impurity would decrease the optical contrast and result in a decrease of the EUV reflectivity and strong increase of the EUVR χ^2. The precise reconstruction of the optical constant profile and especially the optical contrast provides a valuable approach towards comparing multilayer mirror deposition processes [8] and towards predicting the reflectivity of multilayers with different thicknesses or number of periods [9].

8. Conclusion

In conclusion, a simultaneous analysis of both GIXR and EUVR significantly increases the accuracy of the reconstruction of layer densities and material combination compared to GIXR

only analysis. This result will be essential for the use of the reconstructed models for the prediction of EUV reflectivity. The refractive index profiles and their uncertainties can be accurately obtained by GIXRonly data analysis. The addition of EUVR data to the analysis increases the accuracy of the determination of the dimensional parameters. An analysis of correlations indicated that EUVR-only fit will not give an accurate representation of the multilayer periodical structure, and therefore can be used only in combination with GIXR.

Acknowledgments

We acknowledge the support of the Industrial Focus Group XUV Optics at the MESA+ Institute at the University of Twente, notably the industrial partners ASML, Carl Zeiss SMT AG, PANalytical, SolMates, TNO, and Demcon, as well as the Province of Overijssel and the Foundation FOM. Authors also acknowledge the fund supporting Kurchatov Center for Synchrotron Radiation.